ISSN 0029 - 3865

CBPF-NF-074/85

ANGULAR MOMENTUM TRANSFER IN DEEP INELASTIC HEAVY ION COLLISIONS - II

by

V.C. Barbosa[2], P.C. Soares[2], E.C. Oliveira[1] and L.C. Gomes[1]

[1]Centro Brasileiro de Pesquisas Físicas - CBPF/CNPq
Rua Dr. Xavier Sigaud, 150
22290 - Rio de Janeiro, RJ - Brasil

[2]Instituto de Física
Universidade Federal do Rio de Janeiro
Caixa Postal 68528
21941 - Rio de Janeiro, RJ - Brasil

ABSTRACT

The Fokker-Planck equation which describes the angular momentum transfer in deep inelastic heavy ion collisions is solved by a stochastic simulation procedure. The fusion cross section calculation is discussed. The calculations show that the critical orbital angular momentum does not play such an special role as in the deterministic case. The results of the angular momentum transfers and their fluctuations are calculated and compared with experimental results for the reactions $^{86}Kr+^{154}Sm$ at 610 MeV, $^{165}Ho+^{148}Sm$ and $^{165}Ho+^{176}Yb$ at 1400 Mev.

Key-words: Deep inelastic heavy ion reaction.

1 - INTRODUCTION

The use of the Fokker-Planck (F.P.) equation in deep inelastic heavy ion collisions was first proposed by Nörenberg[1]. Since then, the usual procedure for solving this equation has been the expansion of the probabilistic distribution function in its moments up to the second order[2]. Such a procedure is inadequate near the critical angular momentum. This inadequadecy can be easily justified by remembering that the critical angular momentum characterizes an instability region of the underlying deterministic system. This has been exhibited in numerical solutions of the F.P. equation as obtained by Brosa and Cassing[3] for the case of two--dimensional phase space.

In this paper the F.P. equation is solved by a different procedure. We made use of the fact that the results of this equation are the same as predicted by the deterministic system subject to Langevin forces of adequated strengths. In this way, the distribution function was obtained by calculating nearly 18,000 orbits and observing the resulting distributions of the pertinent variables in the asymptotic region. The underlying deterministic system used to describe the reactions is the same of reference 4. The strengths of the Langevin forces were fixed by imposing the Einstein's relations of the brownian motion. The temperature is calculated by imposing that the dissipated energy heats the compound system treated in the free Fermi gas model approximation. The only parameters free to adjust the experimental data are the friction coefficients, already fixed in reference 4. Thus the simulation of the F.P. equation is done without any further adjustments.

We obtained a reasonable agreement with the experimental data for the angular momentum transfer in the reactions $^{86}Kr+^{154}Sm$ at 610 MeV[5], $^{165}Ho+^{148}Sm$ and $^{165}Ho+^{176}Yb$ at 1400 MeV[6]. It is worth mentioning that we did not observe a sharp transition between the deep inelastic and fusion mechanisms when observed as a function of the initial orbital angular momentum (L_0). As a matter of fact in the $^{86}Kr+^{154}Sm$ reaction at 610 MeV for which the critical angular momentum is 197 $\hbar$ the deep inelastic process still compete with the fusion mechanism even for values of the initial orbital angular momentum as low as 40 $\hbar$.

In section 2 we give a brief description of the relations needed for the derivation of the F.P. equation and the method used to fix the temperature. In section 3 we give a description of the actual model employed in the present work and we indicate how to proceed with the simulation. In section 4 we exhibit our results and a discussion is presented in section 5.

2 - THE FOKKER-PLANCK EQUATION

We assume H(q,p) to be the hamiltonian which describes the collective modes of the system that couple to the inelastic channels of a heavy ion collision. The effect of this coupling is assumed to be described by a stochastic force whose mean value gives the friction force and the fluctuating part is taken as a Langevin force. We therefore may write the following equations of motion:

$$\dot{q}^i = \frac{\partial H}{\partial p_i}$$

$$\dot{p}_i = -\frac{\partial H}{\partial q^i} - \Gamma_{ij}\frac{\partial H}{\partial p_j} + \ell_i(t)$$

where Γ_{ij} is the friction coefficient tensor and $\ell_i(t)$ is the Langevin force. We further assume that $\ell_i(t)$ is normally distributed with

$$\langle \ell_i(t) \rangle = 0$$

and

$$\langle \ell_i(t)\ell_j(t') \rangle = 2\,K_{ij}\,\delta(t-t') \quad .$$

Using these assumptions we derive the F.P. equation for $f(q,p;t)$, the probabilistic distribution function for the collective motion of the system[7,8]:

$$\frac{\partial f}{\partial t} + [f,H] = \frac{\partial}{\partial p_i}\left[\Gamma_{ij}\frac{\partial H}{\partial p_j} f + K_{ij}\frac{\partial f}{\partial p_j}\right] \quad .$$

Imposing that the Boltzmann distribution,

$$f(H) = \text{cte.}\; e^{-\frac{H}{T}} \quad ,$$

is the equilibrium solution for the above equation, we obtain the Einstein's relation:

$$K_{ij} = T\,\Gamma_{ij}$$

with T playing the role of the temperature of the system. The temperature of the system is fixed by the relation:

$$U(T) = \int_{-\infty}^{t} \Gamma_{ij}\frac{\partial H}{\partial p_i}\frac{\partial H}{\partial p_j}\,dt'$$

where

$$U(T) = \frac{A}{8} T^2$$

is the internal energy of the compound system treated as a free Fermi gas[9] and A its mass number.

3 - THE SIMULATION

From now on we assume H is given by

$$H = \frac{1}{2\mu} \left(p^2 + \frac{L^2}{r^2}\right) + \frac{J_1^2}{2I_1} + \frac{J_2^2}{2I_2} + V(r)$$

where V(r) is the same potential energy given in reference 4.

The friction coefficient tensor is calculated from a Rayleigh dissipation function F also defined in reference 4 and which we reproduce here:

$$F = \frac{1}{2} \beta \Gamma(r) \left[\dot{r}^2 + \alpha_1 r^2 \left(\dot{\theta} - \frac{R_1}{R_1+R_2} w_1 - \frac{R_2}{R_1+R_2} w_2\right)^2 + \alpha_2 \bar{c}^2 (w_1-w_2)^2\right] .$$

As a direct consequence of the equations of motion the total angular momentum of the collective modes is conserved in the absence of Langevin forces. We will restrict these forces in order to preserve this conservation law. In this way the orbital angular momentum of the system can be obtained from the relation

$$L = L_0 - (J_1 + J_2)$$

where L_0 is the initial angular momentum of the system.

To generate the Langevin forces we integrate the equations of motion by finite differences in steps of $\Delta t = 0.5 \times 10^{-23}$s. At every step the Langevin forces are substituted by random impulses obtained from a normal distribution with zero mean values and covariance matrix (σ_{ij}) given by

$$\sigma_{ij} = 2 K_{ij} \Delta t = 2T \Gamma_{ij} \Delta t \quad .$$

The temperature T in the above equation is calculated along each trajectory using the equation:

$$U(T(t)) = Q^*(t) = - Q(t) + \frac{Q^2(t)}{Q_0}$$

where Q(t) is the energy lost along the orbit. The inclusion of the additional term $Q^2(t)/Q_0$, the energy loss through the vibrational mechanism, is justified in reference 4.

In the case under consideration, we observe that the radial Langevin force is not correlated to the other ones. Therefore we set

$$\Delta p = \sigma_r \cdot U_0$$

with

$$\sigma_r^2 = \sigma_{rr} = 2T \beta \Gamma(r) \Delta t \quad ,$$

where U_0 is a random normal variable of zero mean value and unit variance. The impulses given to J_1 and J_2 can be obtained in a similar way if one takes care of the correlation between them. We have then[10]

$$\Delta J_1 = \sigma_1 . U_1$$

$$\Delta J_2 = \sigma_2 [\rho U_1 + \sqrt{1-\rho^2}\ U_2]$$

with

$$\rho = \frac{\sigma_{12}}{\sigma_1 . \sigma_2}$$

and

$$\sigma_1^2 = \sigma_{11} = [\alpha_1 \left(\frac{R_1}{R_1+R_2}\right)^2 r^2 + \alpha_2 \bar{c}^2] . \sigma_r^2$$

$$\sigma_2^2 = \sigma_{22} = [\alpha_1 \left(\frac{R_2}{R_1+R_2}\right)^2 r^2 + \alpha_2 \bar{c}^2] . \sigma_r^2$$

$$\sigma_{12} = [\alpha_1 \frac{R_1 R_2}{(R_1+R_2)^2} r^2 - \alpha_2 \bar{c}^2] . \sigma_r^2$$

The random variables U_1 and U_2 have the same properties of U_0.

We have simulated an average of 50 orbits for every value of L_0 starting from $L_0 = 40\ \hbar$ to the grazing value for each reaction, in unit steps of $\hbar$. In this way we simulated $\sim 1\times10^4$ orbits for the $^{86}Kr+^{154}Sm$ case, $\sim 2\times10^4$ orbits for the $^{165}Ho+^{148}Sm$ case and $\sim 2.3\times10^4$ orbits for the $^{165}Ho+^{176}Yb$ reaction. For each orbit we stored the asymptotic values of L, J_1, J_2, Q^* and θ . We also kept the collision time for each orbit defining it in such a way as to have zero value in the grazing orbit case.

These data were analyzed with the help of a statistical package in which the statistical weight (W) for each orbit was obtained through the relation:

$$W(b) = \frac{2\pi b \Delta b}{n(L_0)}$$

where $n(L_0)$ is the total number of orbits for the given L_0, b the corresponding impact parameter and Δb the step of b corresponding to $\Delta L_0 = 1\hbar$.

4 - RESULTS

Fig. 1 exhibits the deep inelastic and fusion differential cross sections as a function of the initial angular momentum (L_0) for the $^{86}Kr+^{154}Sm$ reaction at E_{Lab} = 610 MeV. We observe rather small values for the fusion cross sections over the whole L_0 range. Above 220 $\hbar$ and up to 276 $\hbar$ (the grazing value of L_0), the fusion cross section is practically zero. The critical value of L_0 (L_{CR}) in this case is 197 $\hbar$. One observes that the transition of the fusion cross section in the region of L_{CR} is not as abrupt as it could be expected from a deterministic calculation. Therefore, one cannot just take the critical value of the angular momentum to determine the fusion cross section. In our case we adopted a limiting time τ_{FUS} for the deep inelastic mechanism to occur. In Fig. 1 it was taken to be $\tau_{FUS} = 3.5\times10^{-21}$s. This time was obtained through the following argument. In the reaction under consideration the maximum temperature reached by the compound system is approximately 3 MeV. We estimate the single-particle widths at this excitation energy to be close to 210 keV. The corresponding decay time is then approximately equal to 3×10^{-21}s. We take this time as a typical maximum time for the deep inelastic mechanism. The total fusion cross section (σ_{FUS}) predicted by the corresponding deterministic system is 1180 mb. If we had taken $\tau_{FUS} = 2.5\times10^{-21}$s we would have obtained σ_{FUS} = 541 mb. For $\tau_{FUS} = 3.5\times10^{-21}$s we

obtained σ_{FUS} = 244 mb. We observe that σ_{FUS} is rather sensitive to the value of τ_{FUS}. One of the reasons for expecting such a sensitivity is that we make use of the proximity potential energy in our model. This potential energy gives a small binding for the di-nuclear system which easily breaks by the thermal agitation. As a result the longer the value of τ_{FUS} the smaller is σ_{FUS}.

Fig. 2 exhibits the mean value of the total angular momentum transferred to the ions (<J>) as a function of the Q*, for the reaction $^{86}Kr+^{154}Sm$ at 610 MeV of laboratory energy. The open dots were obtained from the experimental data[5] assuming $\langle J_\nu \rangle = 14\ \hbar$. Curves b and c exhibit our results for two different values of τ_{FUS} under the assumption of the rolling mechanism ($\alpha_2 = 0$). One observes that <J> is quite insensitive to the value of τ_{FUS}. Curve a exhibits our results for the sticking mechanism ($\alpha_2 = 0.5$) and $\tau_{FUS} = 3.5\times10^{-21}$s. We observe that the stochastic simulation is somewhat sensitive to the sticking parameter and this hipothesis seems to give a better agreement with the experimental data. A similar effect was not found in the deterministic case[4]. Another point worth mentioning is the fact that the simulated values of <J> goes up to Q* = 250 MeV while in the deterministic case, due to the fusion below $L_{CR} = 197\ \hbar$, we could not obtain predictions of <J> above Q* = 150 MeV.

Fig. 3 shows the standard deviation of the total angular momentum transfer (σ_J) as a function of Q* again in the reaction $^{86}Kr+^{154}Sm$ at 610 MeV. The open dots represents the experimental data[5] assuming $\langle J_\nu \rangle = 14\ \hbar$. Curves b and c correspond to the simulated values for $\tau_{FUS} = 3.5\times10^{-21}$s and $\tau_{FUS} = 2.5\times10^{-21}$s respectively under the rolling assumption ($\alpha_2 = 0$). Contrary to what happen with

<J>, the standard deviation σ_J is more sensitive to the value of τ_{FUS}. Curve a corresponds to the sticking assumption ($\alpha_2 = 0.5$) and $\tau_{FUS} = 3.5\times10^{-21}$s. It is worth mentioning that the sticking assumption contributes both to <J> and σ_J by increasing their values.

In the Figs. 4 and 5 we exhibit both the values <J> and σ_J as a function of Q* for the $^{165}Ho+^{148}Sm$ and $^{165}Ho+^{176}Yb$ reactions at 1400 MeV of laboratory energy. The open dots represent the experimental data[6] for <J> . The simulated data (solid curves) reproduce essentially the deterministic results previously obtained[4].

The results exhibited in Figs. 6,7 and 8 for the case of the reaction $^{165}Ho+^{148}Sm$ at 1400 MeV allow us to discuss the use of Q* as an experimental indicator of the value of L_0. Fig. 6 shows the mean value of L_0 ($<L_0>$) for the simulated (solid curve) and deterministic (dotted curve) cases. The averages were taken over 30 MeV Q* intervals in a way similar to the one utilized to analyze the experimental data. One observes that the two mean values do not differ in any substantial way. Fig. 7 shows the standard deviation of the initial angular momentum (σ_{L_0}) as a function of Q* also for the simulated (solid curve) and deterministic (dotted curve) cases. We observe here that although for the deterministic case the fluctuations lie around 5 $\hbar$ in the simulated case they have values of $\sim$ 40 $\hbar$, i.e. close to ten times larger than in the deterministic case. This suggests that the use of the correlation between Q* and L_0 predicted by the deterministic case should not be taken too seriously. This conclusion is reinforced by the result of the correlation coefficient ($\rho(L_0,Q^*)$) exhibited in Fig. 8. There one observes that for the simulated case the correlation coefficient is small (approximately -0.2) over most of the range of Q*, while for the

deterministic case this coefficient is obviously -1.

5 - CONCLUSIONS

The existence of the critical orbits invalidates the use of expansion in moments of the probabilistic distribution functions near these critical regions of the phase space. The simulated approach is insensitive to such critical regions and its accuracy is dependent only on the amount of available computer time.

For the specific simulation presented here we were able to show that the fusion cross section is insensitive to the critical angular momentum but very sensitive to the maximum time allowed for the di-nuclear system to decay in deep inelastic channels. We believe that this lack of sensitivity has been greatly enhanced by the particular choice of the nuclear potential energy we made. If we had used a potential energy that gives a stronger binding energy to the di-nuclear system, the fusion cross section would have increased, approaching its deterministic value. The lack of experimental values for the fusion cross sections for the reactions studied did not allow us to further study this phenomena. This result can be put in more general terms by saying that the simulated results are sensitive to the value of the transport coefficients over the extended region of the configuration space contrarywise to what happens in the deterministic calculations which are sensitive only to the surface region.

It is worth mentioning that in the way the results were stored we could easily obtain plots of any single or double differential cross section and contour plots of the double differential

cross sections.

The increase of computational facilities created mainly by the advent of microcomputers permits that simulation of stochastic processes such as the one presented here to be done at low cost. In our opinion, simulations such as this one should be carried out in the future for the analysis of experimental data.

We would like to thank Profs. J. Lopes Neto and R. Donangelo for reading the manuscript.

FIGURE CAPTIONS

Fig. 1 - The total (a), the deep inelastic (b) and the fusion (c) differential cross sections as a function of the initial angular momentum for the $^{86}Kr+^{154}Sm$ reaction at 610 MeV. The horizontal scale is the initial angular momentum in units of $\hbar$ ($L_0 = \ell_0\hbar$). The vertical scale is the $d\sigma/d\ell_0$ in mb. The fusion cross section was obtained by assuming a maximum limiting time $\tau_{FUS} = 3.5\times10^{-21}$s and under the rolling assumption ($\alpha_2 = 0$).

Fig. 2 - The mean total angular momentum transfer <J> in the $^{86}Kr+^{154}Sm$ reaction as a function of the energy loss (Q*). The horizontal scale is Q* in units of MeV and the vertical scale is the mean total angular momentum transfer in units of $\hbar$. The open dots are the experimental data of reference 5 assuming $<J_\nu>= 14\ \hbar$. Curve a is the prediction of our model with the sticking assumption ($\alpha_2 = 0.5$) and $\tau_{FUS} = 3.5\times10^{-21}$s. Curves b and c are the same as a but under the assumption of rolling mechanism. Curve b assumes $\tau_{FUS} = 3.5\times10^{-21}$s and curve c $\tau_{FUS} = 2.5\times10^{-21}$s.

Fig. 3 - The same as Fig. 2 but refering to the standard deviation of the angular momentum transfer in the $^{86}Kr+^{154}Sm$ reaction.

Fig. 4 - The mean value <J> and the standard deviation σ_J of the total angular momentum transfer as a function of Q* for the $^{165}Ho+^{148}Sm$ reaction at 1400 MeV. The open dots are the experimental data for <J> of reference 6. The two curves are our results for the <J> (solid curve) and σ_J (dotted curve). The horizontal and vertical scales are the same as in Fig. 2.

Fig. 5 - The same as Fig. 4 but for the $^{165}Ho+^{176}Yb$ reaction at 1400 MeV.

Fig. 6 - The mean of the initial angular momentum as a function of Q* for the $^{165}Ho+^{148}Sm$ reaction. The mean values were taken for every 30 MeV Q* intervals. The solid curve refers to the simulated and the dotted one to the deterministic calculations. The horizontal and vertical scales are the same as in Fig. 2.

Fig. 7 - The standard deviation of the initial angular momentum, for 30 MeV Q* intervals, as a function of Q* for the same reaction of Fig. 6. The horizontal and vertical scales are the same as in Fig. 2. The solid curve corresponds to the simulated and the dotted one to the deterministic calculations.

Fig. 8 - The correlation coefficient of the L_0Q^* pair of variables as a function of Q* for the same reaction used in Figs. 6 and 7. The horizontal scale is in units of MeV.

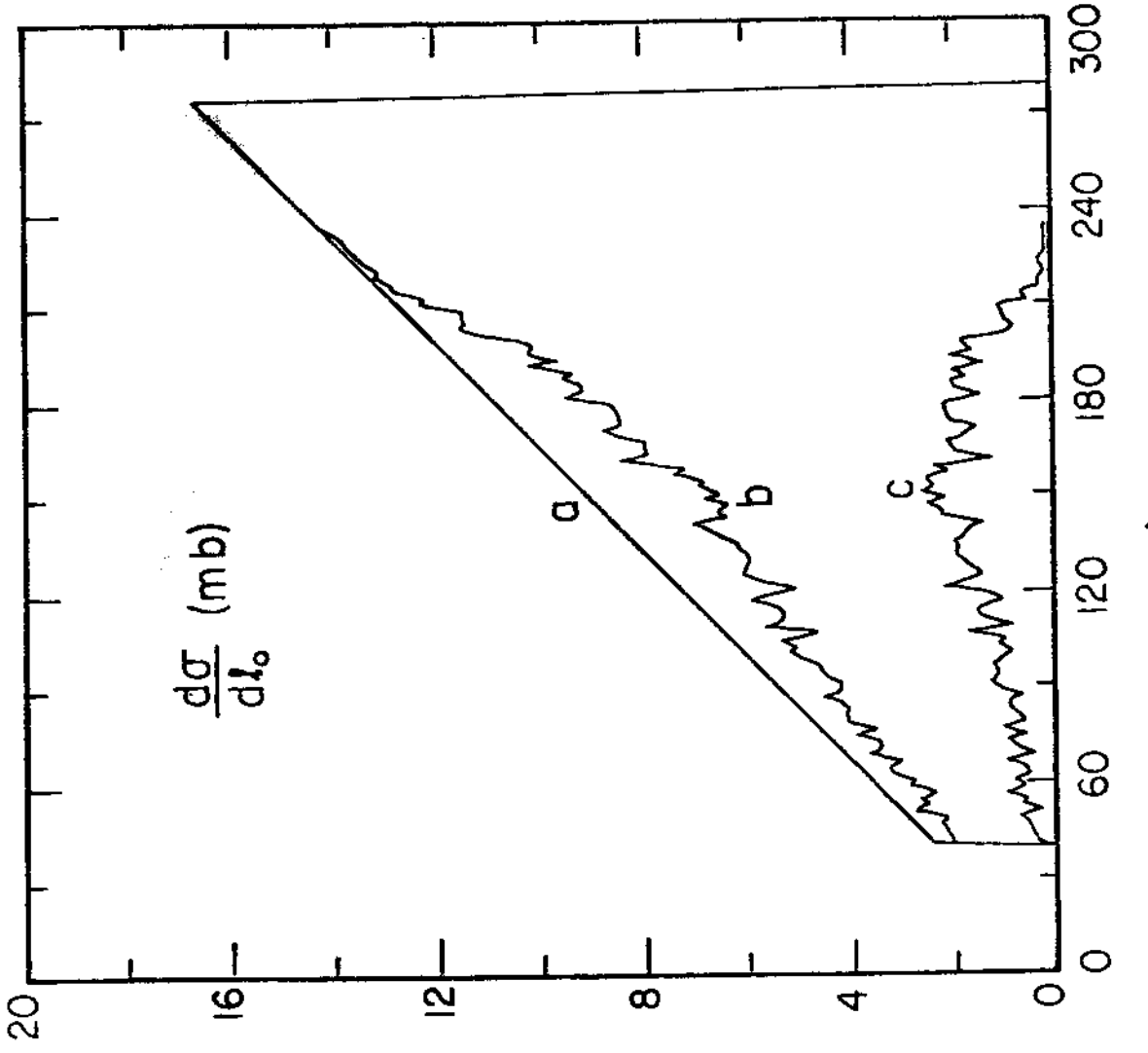

FIG. 1

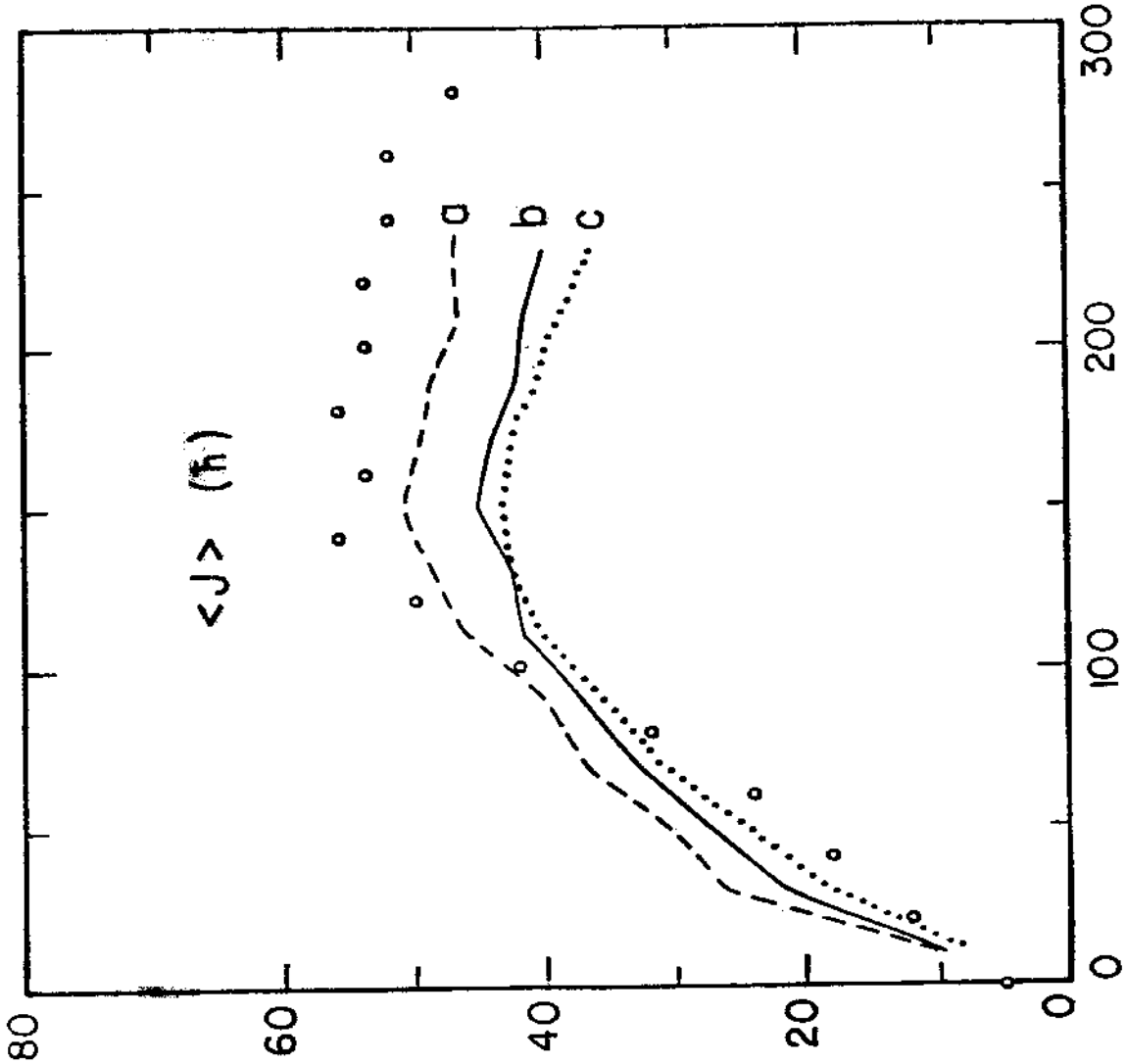

FIG. 2

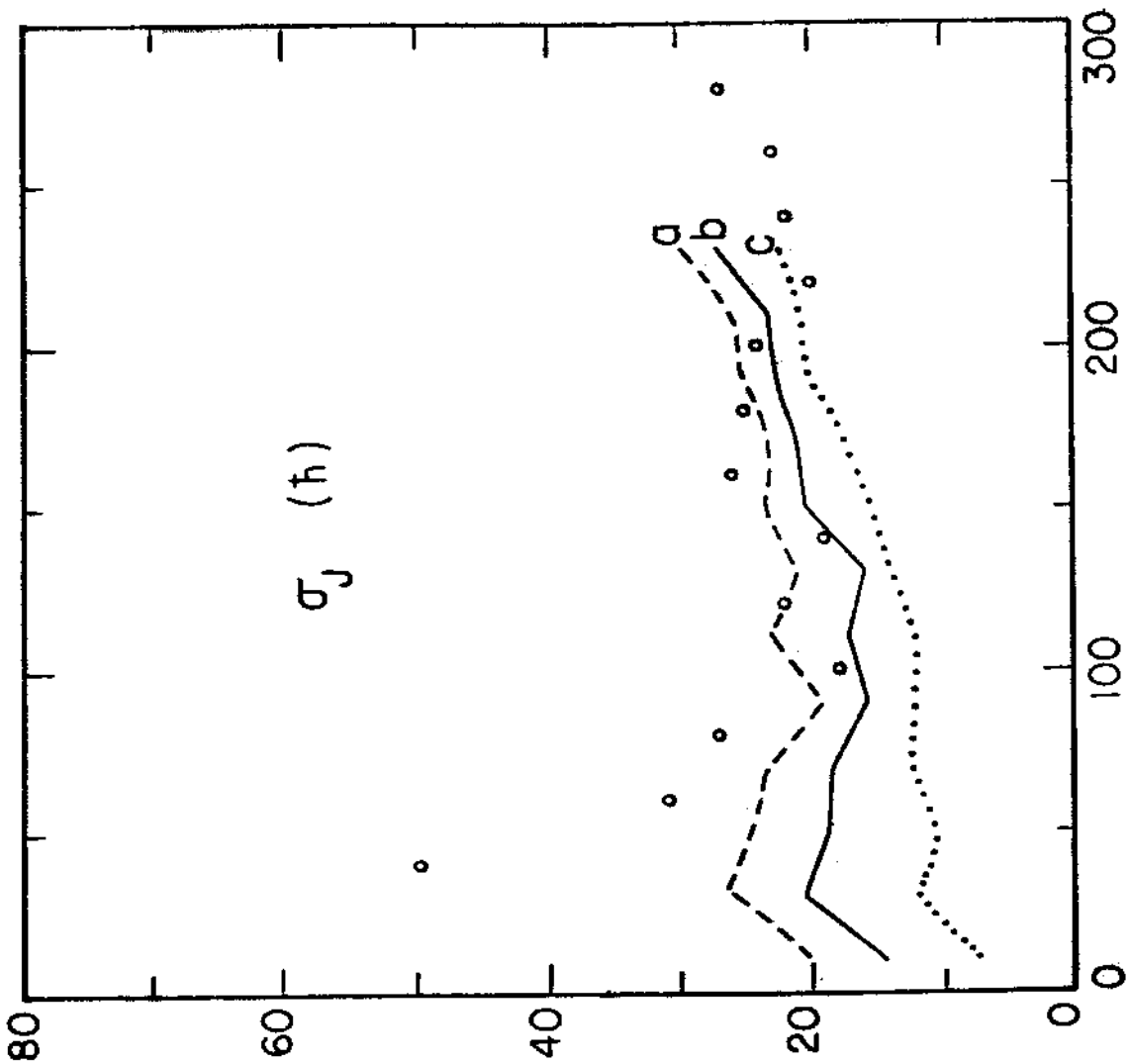

FIG. 3

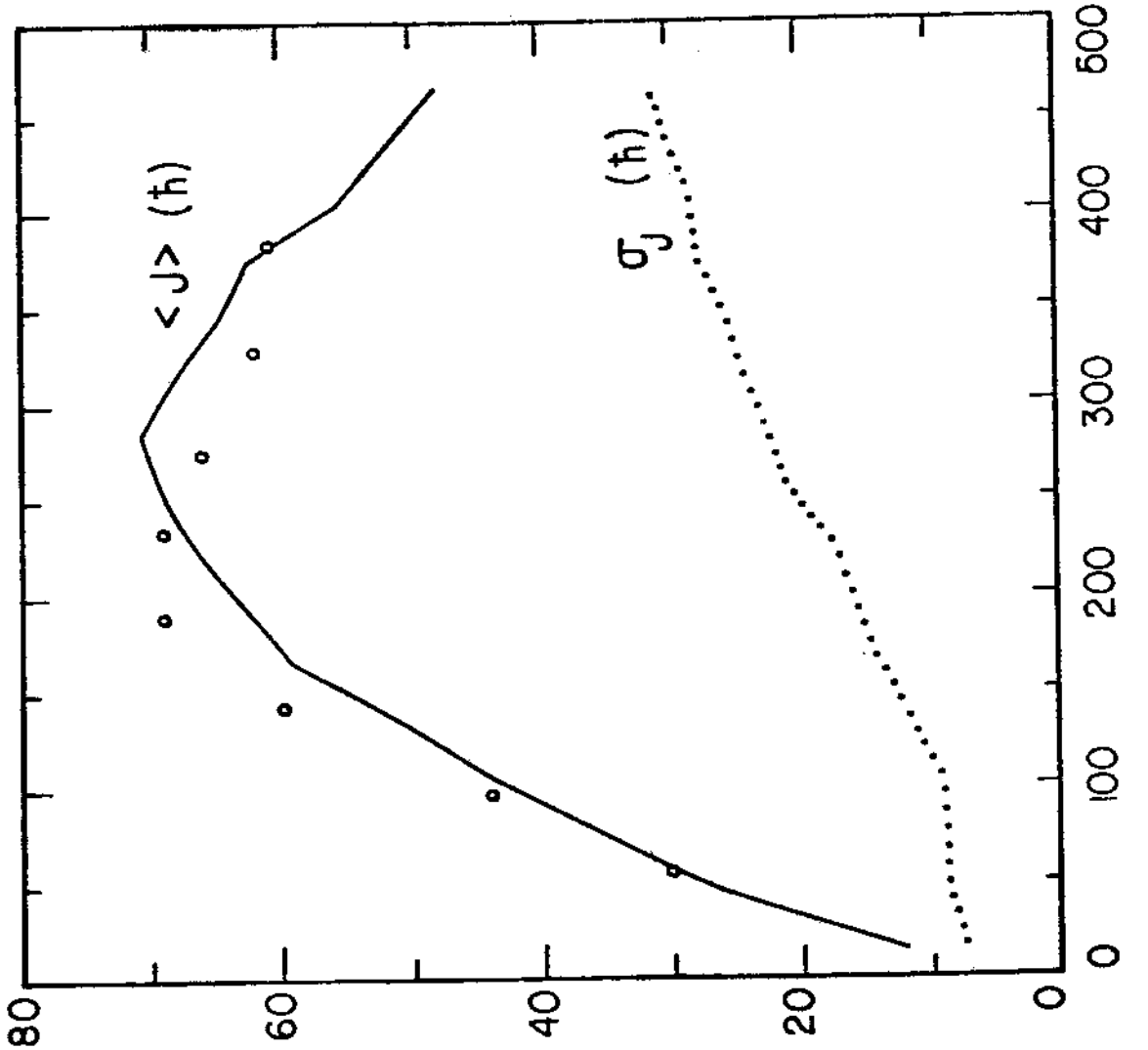

FIG. 4

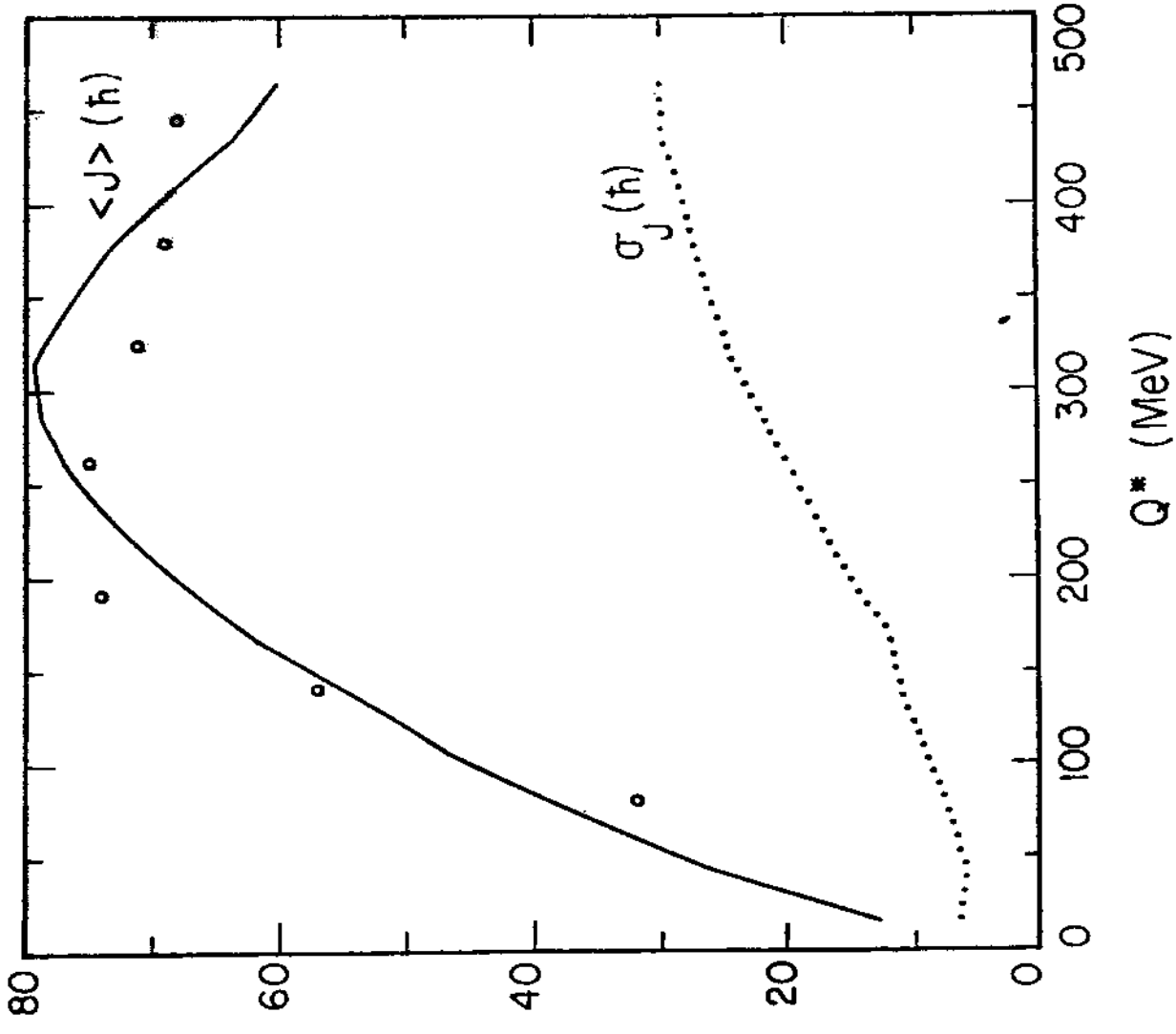

FIG. 5

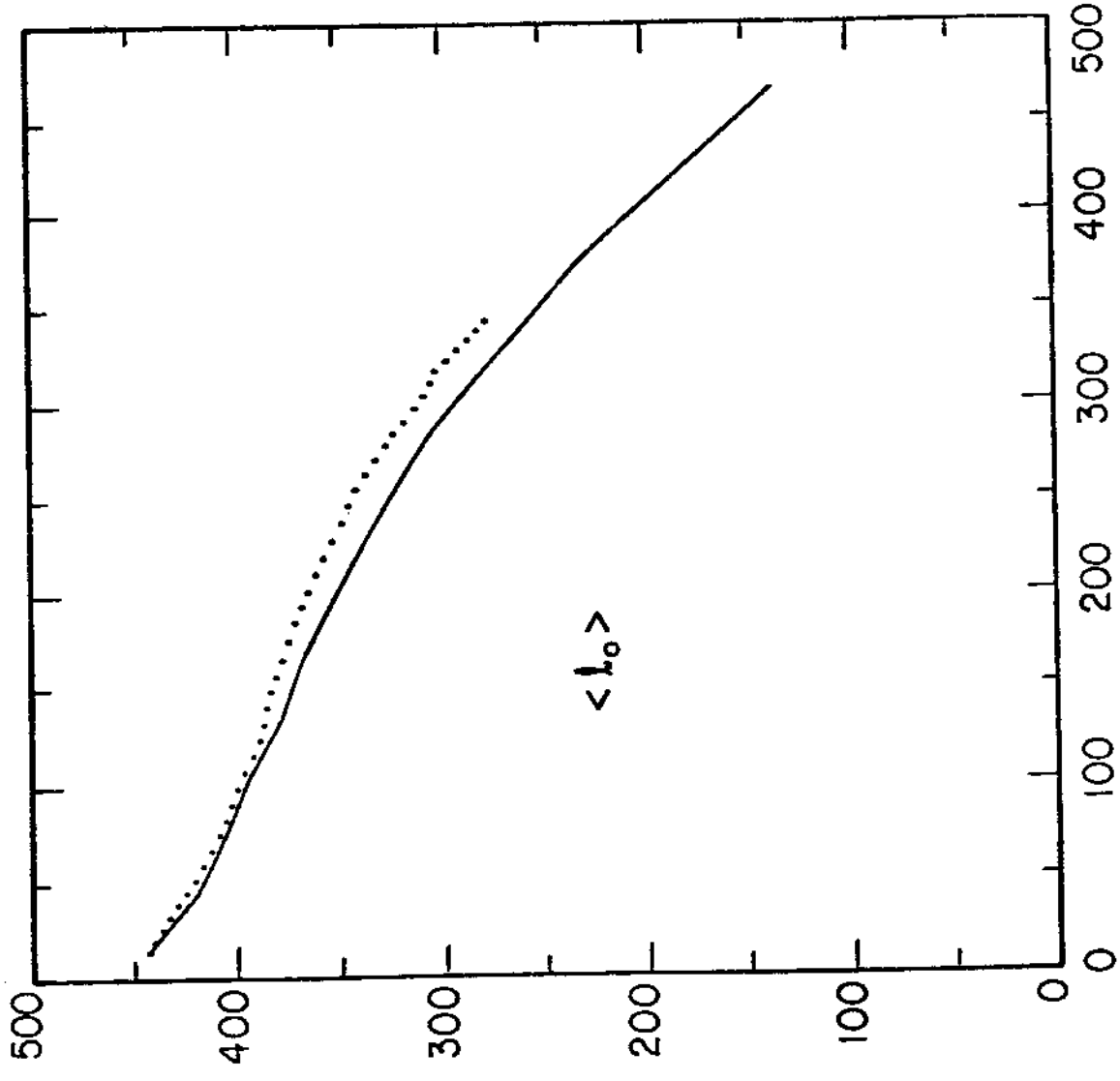
500
400
300
200
100
0
0
100
200
300
400
500
Q* (MeV)
<l₀>
FIG. 6

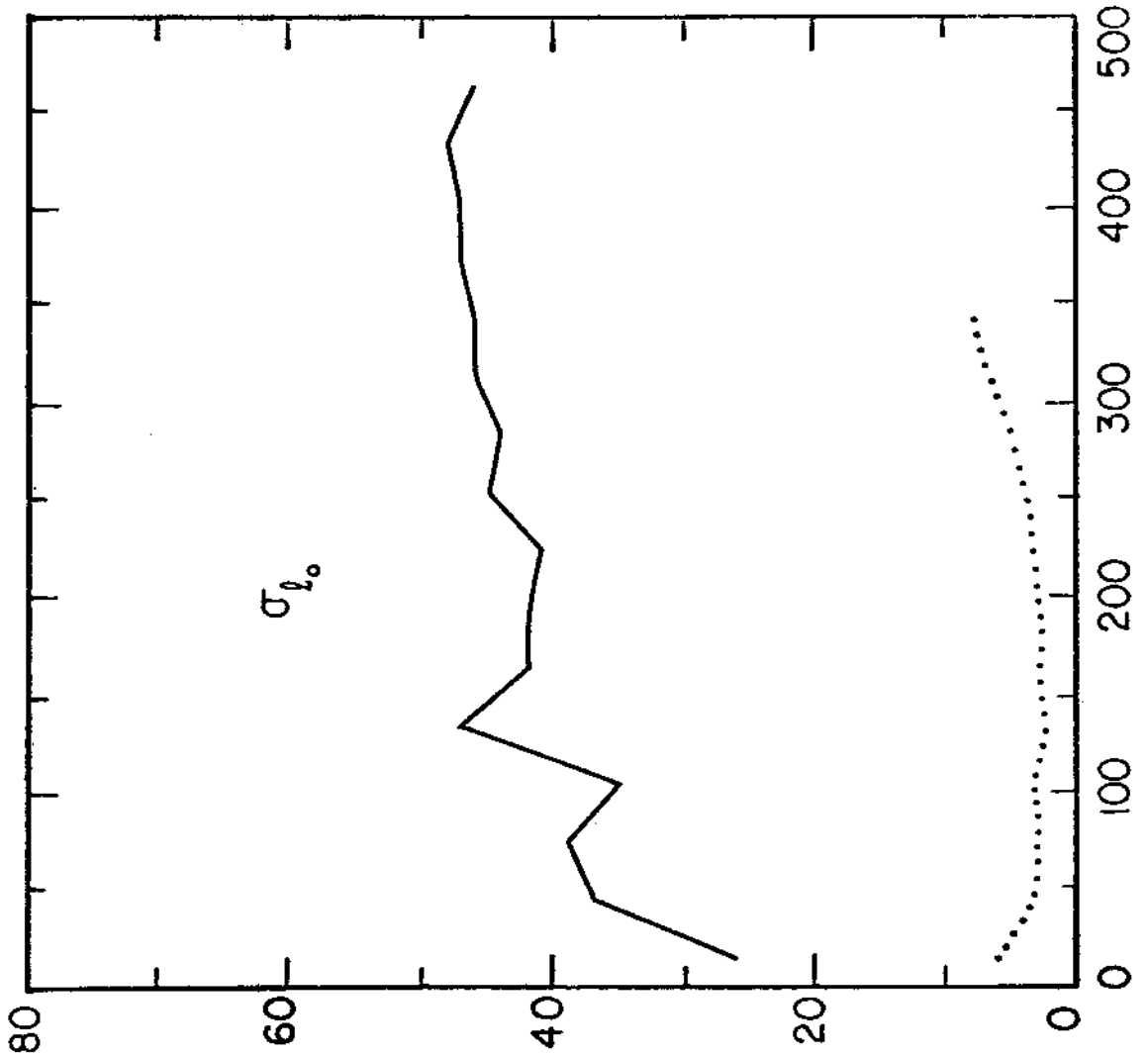

FIG. 7

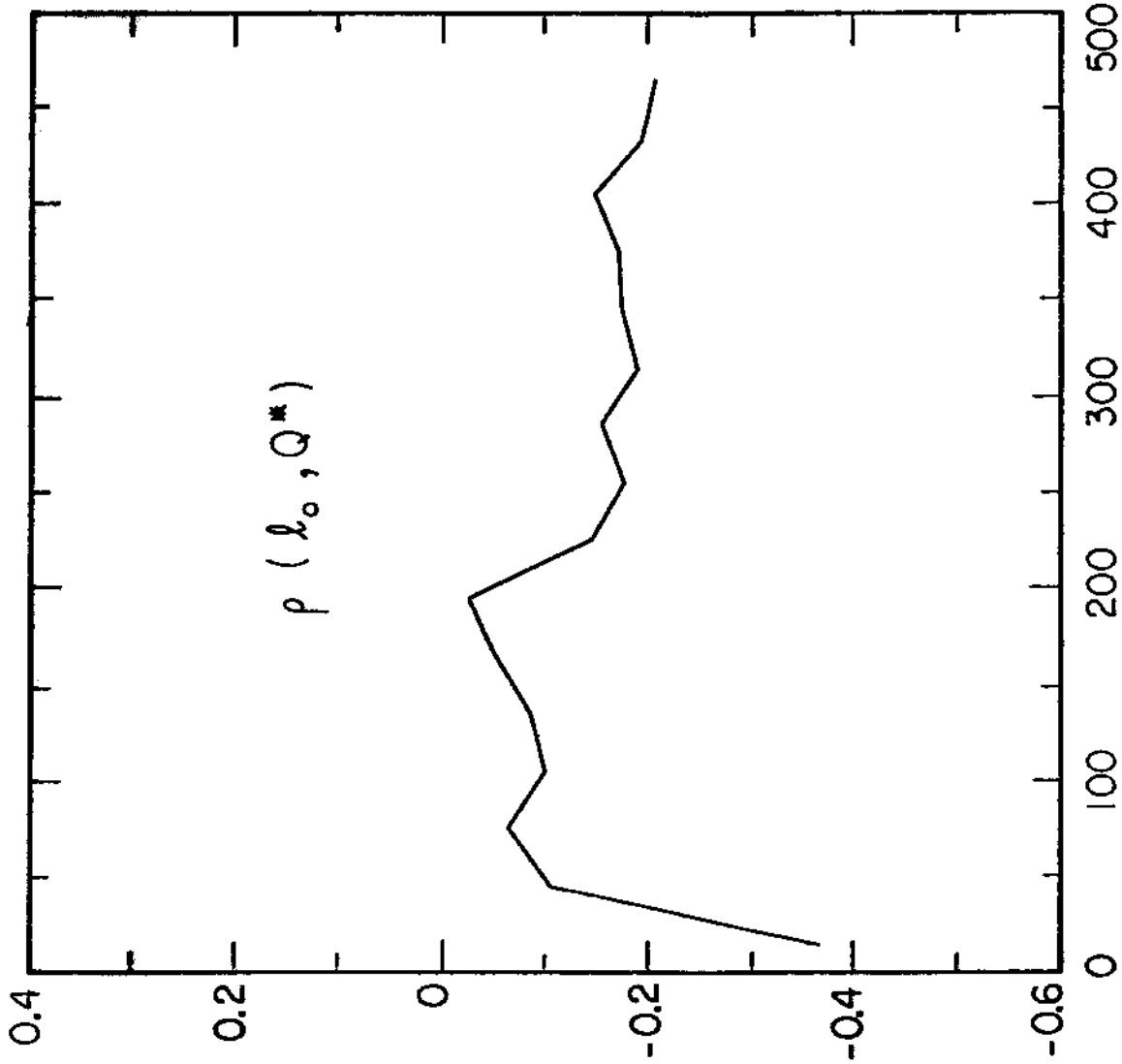

FIG. 8

REFERENCES

1 - Nörenberg (W.): Phys. Lett. 52B(1974)289.

2 - Ngô (C.), Hofmann (H.): Z. Phys. A282(1977)83.
Berlanger (M.), Ngô (C.), Grangé (P.), Richert (J.), Hofmann (H.): Z. Phys. A284(1978)61.
Riedel (C.), Wolschin (G.): Z. Phys. A 294(1980)167.

3 - Brosa (U.), Cassing (W.): Z. Phys. A307(1982)167.

4 - Barbosa (V.C.), Carrilho Soares (P.), Oliveira (E.C.), Gomes (L.C.): Rev. Bras. Fís. 14(1984)337.

5 - Christensen (P.R.), Ole Hansen, Nathan (O.), Videbaek (F.), Freiesleben (H.), Britt (H.C.), van der Werf (S.Y.): Nucl. Phys. A390(1982)336.

6 - Pacheco (A.J.), Wozniak (G.J.), McDonald (R.J.), Diamond (R.M.), Hsu (C.C.), Moretto (L.G.), Morrissey (D.J.), Sobotka (L.G.), Stephens (F.S.): Nucl. Phys. A397(1983)313.

7 - Balescu (R.): Equilibrium and Nonequilibrium Statistical Mechanics, John Wiley and Sons, New York (1975).

8 - Nix (J.R.): Nuclear Dissipation in Heavy-Ion Reactions and Fission - Preprint LA-UR-82-3651 (1982).

9 - Bohr (Aa.), Mottelson (B.R.): Nuclear Structure - Volume I, W.A. Benjamin, New York (1969).

10 - Abramowitz (M.), Stegun (I.A.) (eds.): Handbook of Mathematical Functions, Dover Publications, New York (1970).